

## **Final Performance Report**

**Project Title:** Highly Efficient Organic Photovoltaic Cells from  
Polymer-Aligned Carbon Nanotube Dispersed  
Heterojunctions

**Contract Number:** AFOSR (FA9550-06-1-0384)

**Report Title:** Final Performance Report

**Report Period:** March, 2006 – September, 2009

**Funding Organization:** AFOSR

**Prepared by:** Dr. Liming Dai  
Principal Investigator  
University of Dayton  
300 College Park  
Dayton, OH 45469-0104  
Tel: (937) 229 2670  
[ldai@udayton.edu](mailto:ldai@udayton.edu)

**Prepared for:** Dr. Charles Lee  
AFOSR/NA  
875 North Randolph Street  
Suite 325, Room 3112  
Alexandria, VA 22203  
(703) 696-7779  
[charles.lee@afosr.af.mil](mailto:charles.lee@afosr.af.mil)

REPORT DOCUMENTATION PAGE					Form Approved OMB No. 0704-0188	
<p>The public reporting burden for this collection of information is estimated to average 1 hour per response, including the time for reviewing instructions, searching existing data sources, gathering and maintaining the data needed, and completing and reviewing the collection of information. Send comments regarding this burden estimate or any other aspect of this collection of information, including suggestions for reducing the burden, to Department of Defense, Washington Headquarters Services, Directorate for Information Operations and Reports (0704-0188), 1215 Jefferson Davis Highway, Suite 1204, Arlington, VA 22202-4302. Respondents should be aware that notwithstanding any other provision of law, no person shall be subject to any penalty for failing to comply with a collection of information if it does not display a currently valid OMB control number.</p> <p><b>PLEASE DO NOT RETURN YOUR FORM TO THE ABOVE ADDRESS.</b></p>						
1. REPORT DATE (DD-MM-YYYY) 20-10-2009		2. REPORT TYPE Final Performance Report			3. DATES COVERED (From - To) March 2006 - September 2009	
4. TITLE AND SUBTITLE Highly Efficient Organic Photovoltaic Cells from Polymer-Aligned Carbon Nanotube Dispersed Heterojunctions					5a. CONTRACT NUMBER FA9550-06-1-0384	
					5b. GRANT NUMBER	
					5c. PROGRAM ELEMENT NUMBER	
					5d. PROJECT NUMBER	
6. AUTHOR(S) Liming Dai					5e. TASK NUMBER	
					5f. WORK UNIT NUMBER	
7. PERFORMING ORGANIZATION NAME(S) AND ADDRESS(ES)  University of Dayton (University of Dayton Research Institute) 300 College Park					8. PERFORMING ORGANIZATION REPORT NUMBER	
9. SPONSORING/MONITORING AGENCY NAME(S) AND ADDRESS(ES)  Dr. Charles Lee AFOSR/NA 875 North Randolph Street Suite 325, Room 3112					10. SPONSOR/MONITOR'S ACRONYM(S)	
					11. SPONSOR/MONITOR'S REPORT NUMBER(S)	
12. DISTRIBUTION/AVAILABILITY STATEMENT Distribution public release						
13. SUPPLEMENTARY NOTES						
14. ABSTRACT  As we proposed originally, we have focused on the syntheses of novel vertically-aligned carbon nanotube arrays and conjugated macromolecules for photovoltaic cells. Towards this effort we have developed new synthetic methods for the growth of vertically-aligned single-walled carbon nanotubes (VA-SWNTs), semiconducting VA-SWNTs, and multicomponent micropatterns of VA-CNTs. We also designed and synthesized several classes of novel low bandgap photovoltaic active polymers, and polymer-/TiO <sub>2</sub> -coated VA-CNTs, critical to developing high efficient polymer photovoltaic cells and dye-sensitized solar cells. Polymer photovoltaic cells with 3-D structural features, including bilayer-/homotropically-aligned bulk-heterojunctions, were also developed for an efficient solar absorption and charge separation/collection. Besides, novel N-doped CNT fuel cells, polymer/quantum dot light-emitting diodes, and even CNT Gecko-foot-mimetic dry adhesives, were developed for energy management. This project has led to about 30 journal publications, including two Science and one Nature Nanotechnology papers, and a joint patent application with Wright Patterson Air Force Base.						
15. SUBJECT TERMS Photovoltaic polymers, Aligned carbon nanotubes, Solar cells, Fuel cells, LEDs, Dry adhesives						
16. SECURITY CLASSIFICATION OF:			17. LIMITATION OF ABSTRACT	18. NUMBER OF PAGES	19a. NAME OF RESPONSIBLE PERSON	
a. REPORT	b. ABSTRACT	c. THIS PAGE			19b. TELEPHONE NUMBER (Include area code)	
unclassified	unclassified	unclassified	SAR			

## ABSTRACT

As we proposed originally, we have focused on the syntheses of novel vertically-aligned carbon nanotube arrays and conjugated macromolecules for photovoltaic cells. Towards this effort we have developed new synthetic methods for the growth of vertically-aligned single-walled carbon nanotubes (VA-SWNTs), semiconducting VA-SWNTs, and multicomponent micropatterns of VA-CNTs. We also designed and synthesized several classes of novel low bandgap photovoltaic active polymers, and polymer-/TiO<sub>2</sub>-coated VA-CNTs, critical to developing high efficient polymer photovoltaic cells and dye-sensitized solar cells. Polymer photovoltaic cells with 3-D structural features, including bilayer-/homotropically-aligned bulk-heterojunctions, were also developed for an efficient solar absorption and charge separation/collection. Besides, novel N-doped CNT fuel cells, polymer/quantum dot light-emitting diodes, and even CNT Gecko-foot-mimetic dry adhesives, were developed for energy management. This project has led to about 30 journal publications, including two *Science* and one *Nature Nanotechnology* papers, and a joint patent application with Wright-Patterson Air Force Base.

# TABLE OF CONTENTS

<b>I. ACCOMPLISHMENTS AND NEW FINDINGS.....</b>	<b>4</b>
<b>A. SUMMARY OF ACCOMPLISHMENTS ON MATERIALS SYNTHESSES.....</b>	<b>4</b>
1 PHOTOVOLTAIC MACROMOLECULES.....	4
1.1 Photoactive dendrimers.....	4
1.2 Dithienosilole-containing Low Bandgap Polymers .....	4
1.3 Donor- -Acceptor Photovoltaic-active Copolymers Based On Thiophene (donor) and 2-pyran-4-ylidene-malononitrile (acceptor) .....	5
2 MULTICOMPONENT MICROPATTERNS OF VA-CNTs.....	6
2.1 VA-SWNTs and VA-MWNTs Interposed Multicomponet Micropatterns .....	6
2.2 Multicomponent and Multidimensional CNT Micropatterns by Dry Contact Transfer.....	6
2.3 VA-CNTs Functionalized with Titanium Dioxide.....	8
2.4 Semiconducting VA-SWNTs.....	9
2.5 Smart Polymer and VA-CNTs Composites.....	10
<b>B. SUMMARY OF ACCOMPLISHMENTS ON DEVICES.....</b>	<b>11</b>
3 PHOTOVOLTAIC CELLS.....	11
3.1 Photovoltaic Cells Based on Dithienosilole-containing Polymers.....	11
3.2 Photovoltaic Cells Based on D- -A Conjugated Copolymers.....	12
3.3 Photovoltaic Cells Based on Liquid Crystalline Liscon.....	12
3.4 Photovoltaic Cells Based on Liquid Crystalline Porphyrins.....	13
3.5 Photovoltaic Cells Based on VA-CNTs.....	14
<b>C. OTHER ENERGY-RELATED DEVICES.....</b>	<b>15</b>
4.1 White Polymer LEDs.....	15
4.2 QD-LEDs.....	15
4.3 Fuel Cells.....	16
4.4 Dry Adhesives.....	17
<b>II. JOURNAL PUBLICATIONS AND PATENTS .....</b>	<b>18</b>
<b>III. PERSONNEL SUPPORT.....</b>	<b>20</b>
<b>IV. SIGNIFICANCE.....</b>	<b>21</b>
<b>V. INTERACTIONS.....</b>	<b>21</b>

## I. ACCOMPLISHMENTS AND NEW FINDINGS

### A. SUMMARY OF ACCOMPLISHMENTS ON MATERIALS SYNTHESSES

#### 1 SYNTHESSES OF NOVEL PHOTOVOLTAIC ACTIVE CONJUGATED MACROMOLECULES

##### 1.1 Syntheses of Novel Photovoltaic dendrimers (*J. Mater. Chem.* **2007**, 17, 364; *Nanotechnology* **2007**, 18, 365605)

A class of new dendrimers consisting of hydrophobic oligo(*p*-phenylene vinylene) core branches and hydrophilic oligo(ethylene oxide) terminal chains have been synthesized (Figure 1). These amphiphilic dendritic molecules are highly luminescent and exhibit novel temperature-responsive phase behaviors with reversible changes in photophysical properties and some interesting photovoltaic effects.

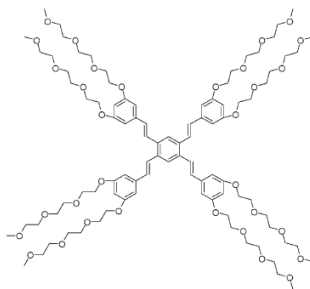
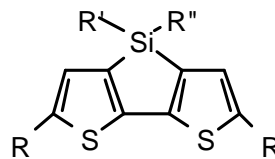
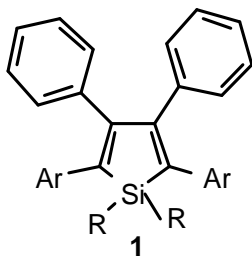


**Figure 1.** Molecular structures of amphiphilic dendrimers with oligo(*p*-phenylene vinylene) core branches and oligo(ethylene oxide) terminal chains<sup>5</sup>.

##### 1.2 Syntheses of Dithienosilole-containing Low Bandgap Photovoltaic-active Polymers (*Macromolecules* **2009**, 42, 114)

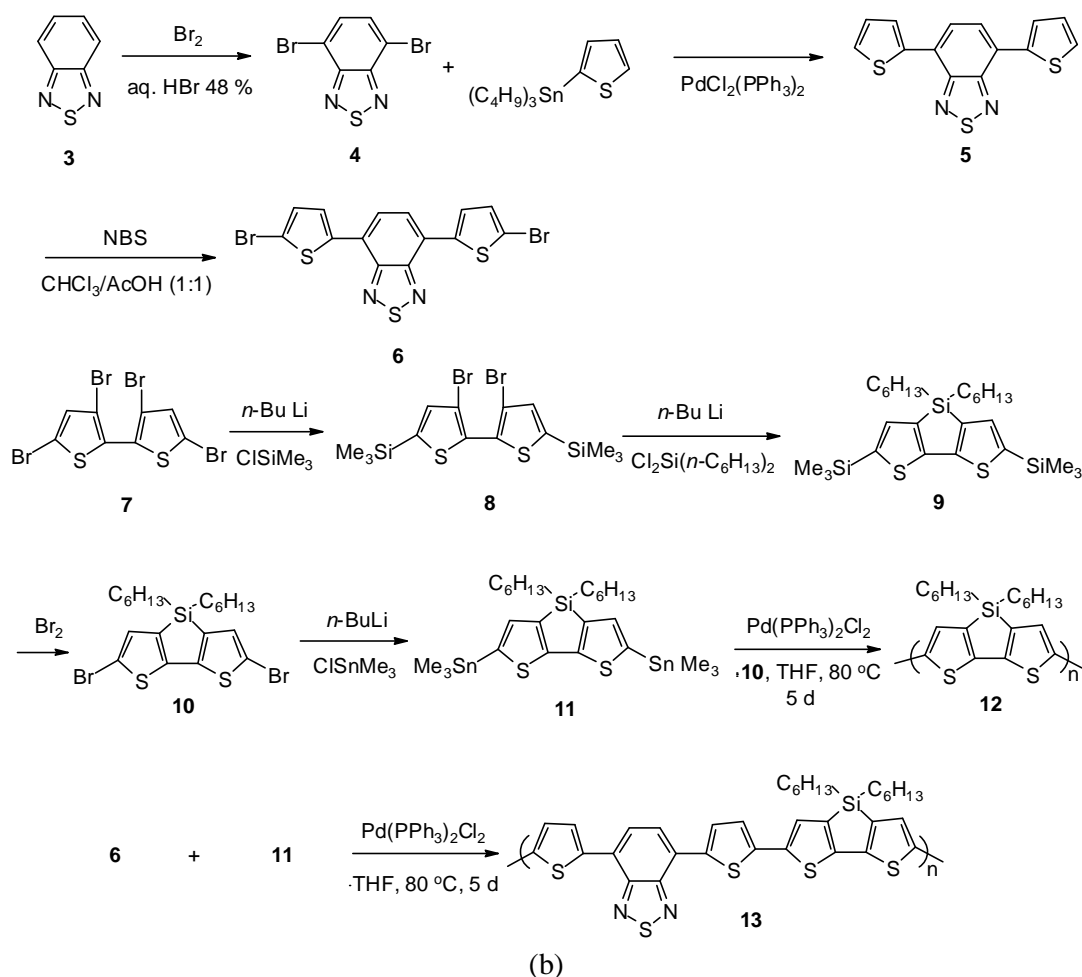
Silole-containing polymers consisting of a dithienosilole homopolymer backbone (**12**) or an alternating dithienosilole and 4,7-bis(-2-thienyl)-2,1,3-benzothiadiazole copolymer backbone (**13**) were synthesized via Scheme 1. The presence of planar dithienosilole tricyclic units along these - conjugated polymer backbones lowered the band gap and led to strong absorption in the visible region of the solar spectrum. The introduction of electron-withdrawing benzothiadiazole moieties along the dithienosilole backbone further reduced the optical bandgap and increased the interchain interaction. Bulk-heterojunction organic solar cells using 1:1 w/w polymer **12** or **13**:PCBM (methanofullerene [6,6]-phenyl C61-butyric acid methyl ester) blends as the photoactive layers were prepared. Photovoltaic cells with copolymer **13** as the electron donor and PCBM as the electron acceptor exhibited an increased energy conversion efficiency by a factor of 3 under an AM 1.5 simulated solar light at 100 mW/cm<sup>2</sup> after thermal annealing at 140 °C (Section B). This is one of the very first silole-containing polymers synthesized for photovoltaic applications.



**2 a** DTS, R=H

**b** DTsBr<sub>2</sub>, R=Br

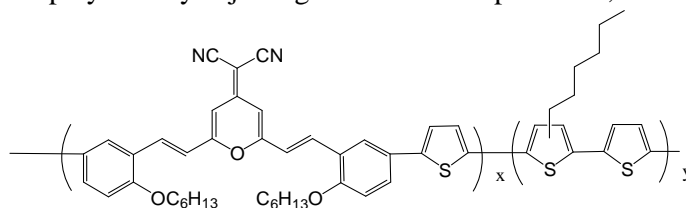
(a)



**Scheme 1.** Syntheses and structures of -containing polymers **12** and **13**.

### 1.3 Donor- -Acceptor Photovoltaic-active Copolymers Based On Thiophene (donor) and 2-pyran-4-ylidene-malononitrile (acceptor) (*J. Phys. Chem. B* **2008**, 112, 2801)

A class of new conjugated copolymers containing donor (thiophene)-acceptor (2-pyran-4-ylidene-malononitrile, PYM) was synthesized *via* Stille coupling polymerization (Figure 2). UV-vis spectra indicated that the increase in the content of thiophene units increased the interaction between the polymer main chains to cause a red-shift in the optical absorbance. Both the experimental and DFT calculation results indicated an increase in the HOMO energy level with increasing the content of thiophene units, whereas the corresponding change in the LUMO energy level is much smaller. These results provided a novel concept for developing high  $V_{oc}$  photovoltaic cells based on donor- $\pi$ -acceptor conjugated copolymers by adjusting the donor/acceptor ratio, to be discussed in Section B).



**Commonmer ratio:**  $x:y=1:0$ (P1),  $x:y=0.8:0.2$ (P2),  $x:y=0.5:0.5$ (P3)

**Figure 2.** Molecular structures of (a) amphiphilic dendrimers with oligo(*p*-phenylene vinylene) core branches and oligo(ethylene oxide) terminal chains, (b, c) dithienosilole-containing conjugated polymers and D- -A conjugated polymers.

## 2 CONTROLLED PREPARATION OF MULTIDIMENSIONAL AND MULTI-COMPONENT MICROPATTERNS OF ALIGNED CARBON NANOTUBE ARRAYS

### 2.1 Direct Growth Of Multicomponent Micropatterns Of Vertically-aligned Single-walled Carbon Nanotubes Interposed with Their Multiwalled Counterparts (J. Mater. Chem. **2007**, 17, 3401; Cover page publication)

We have developed a facile but effective method for synthesizing vertically-aligned single-walled carbon nanotube (VA-SWNT) arrays. On this basis, we have further demonstrated the first direct growth of multicomponent micropatterns of VA-SWNTs interposed within the patterned areas surrounded by vertically-aligned multi-walled carbon nanotubes (VA-MWNTs) onto an Al-activated iron substrate (Figure 3). The Al-activated iron substrate was prepared by region-selectively depositing an Al thin layer on either an Fe-coated substrate or a commercially-available iron foil. To directly grow aligned carbon nanotubes on metallic (conducting) substrates is of practical importance, especially for fabricating nanotube-based electronic devices. The methodology developed in this work allows for an effective integration of various aligned carbon nanotubes with different electronic characteristics into multifunctional materials and devices.

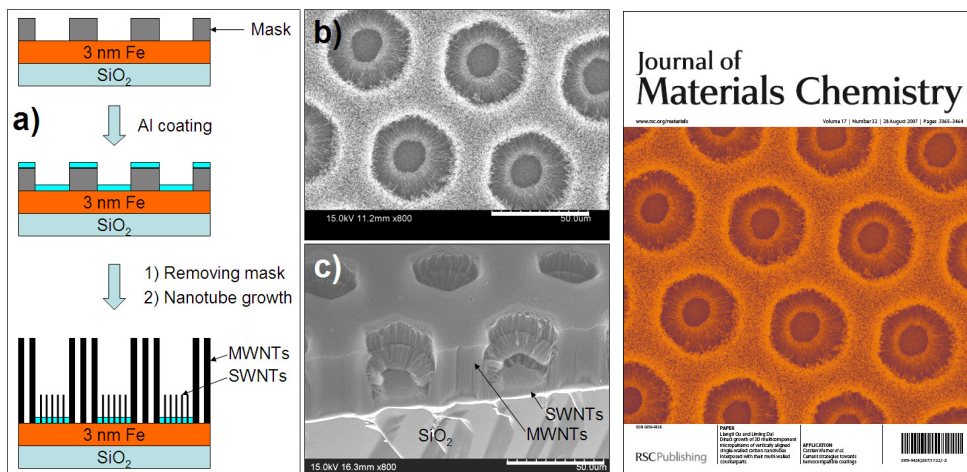


**Figure 3.** a) Schematic representation of Al patterning on an Fe-coated substrate for the patterned growth of three-dimensional interposed VA-SWNTs and VA-MWNTs. b, c) Top and cross-section views of the VA-MWNT/VA-SWNT micropatterns. Scale bars: 50  $\mu\text{m}$ . d) A typical SEM image of the VA-MWNT/VA-SWNT micropattern published as a cover page in *Journal of Materials Chemistry*.

### 2.2 Multicomponent and Multidimensional Carbon Nanotube Micropatterns by Dry Contact Transfer (J. Nanosci. Nanotechnol. **2007**, 7, 1573; *Appl. Phys. Lett.* **2006**, 89, 103103)

We have also prepared multicomponent micropatterns with silica particles interposed within the discrete areas surrounded with micropatterned VA-MWNTs by dry contact transferring aligned carbon nanotubes onto a Scotch tape pre-patterned with a thin layer of gold structure, followed by region-specific adsorption of thiol-modified silica particles onto the gold surface from solution (Figure 4a&b). The dry contact transfer technique, in conjunction with aligned carbon nanotube growth, has further enabled us to develop micropatterns of aligned single-wall carbon nanotubes with interdispersed non-aligned multiwall carbon nanotubes, and micro-sized carbon fibers sheathed with micropatterned aligned carbon nanotubes (Figure 4c&d). These results represent significant advances in the development of various new multi-dimensional and multifunctional nanomaterials attractive for a wide range of device applications, including advanced photovoltaic cells.

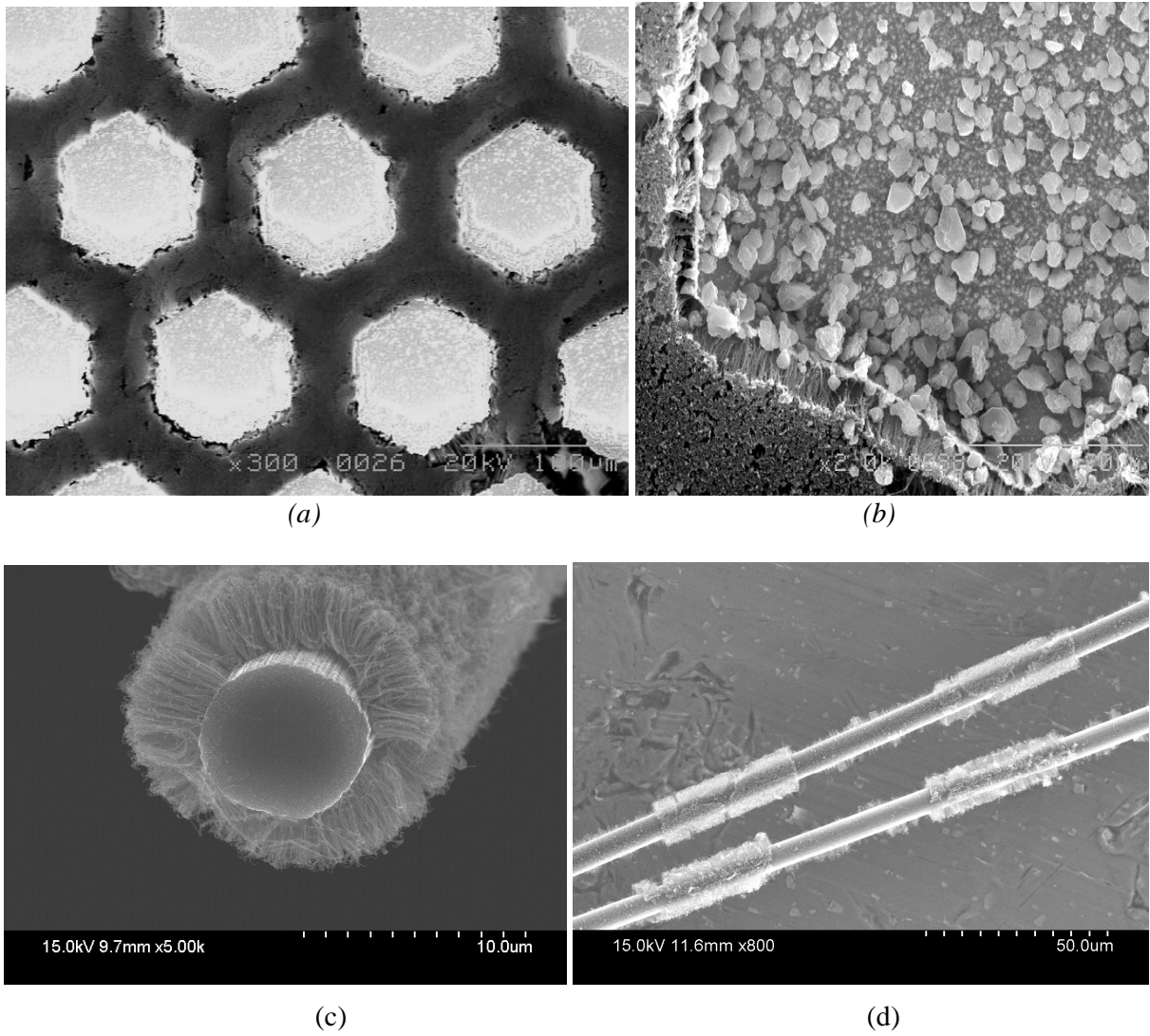


**Figure 4.** SEM images of (a) the multicomponent interposed carbon nanotube micropatterns with nonspherical silica particles region-specifically adsorbed onto the gold surfaces interdispersed within the aligned carbon nanotube patterns (scale bar: 100 μm), (b) a high magnification image as for (a) (scale bar: 20 μm), (c) a cross-section view of the carbon fiber and nanotube hybrid structure, showing the perpendicularly-aligned nanotubes surrounding the microfiber, and (d) carbon microfibers sheathed with micropatterned aligned carbon nanotubes by the dry contact transfer technique.

We have further used the dry contact transfer technique for controlled preparation of three-dimensional perpendicularly-aligned carbon nanotube micropatterns with region-specific tube lengths. In this case, we first sputter-coated a micropatterned metal (*e.g.* Al, Ag, Au) layer onto the *as-synthesized* VA-MWNT array of a uniform nanotube length (*left of Figure 5a*), followed by pressing an adhesive film (*e.g.* a 3M Scotch tape) onto the VA-MWNT array pre-patterned with the metal layer (*top right of Figure 5a*), peeling off the Scotch tape with the VA-MWNT film from the quartz substrate in a dry state, turning over the Scotch-supported ACNT film upside down (*middle right of Figure 5a*), and pushing up the Scotch tape underneath the metal-patterned area against the rest part of the VA-MWNT film (*bottom right of Figure 5a*) to produce the 3-dimensional (3-D) VA-MWNT micropatterns with a region-specific tube length (Figure 5b).

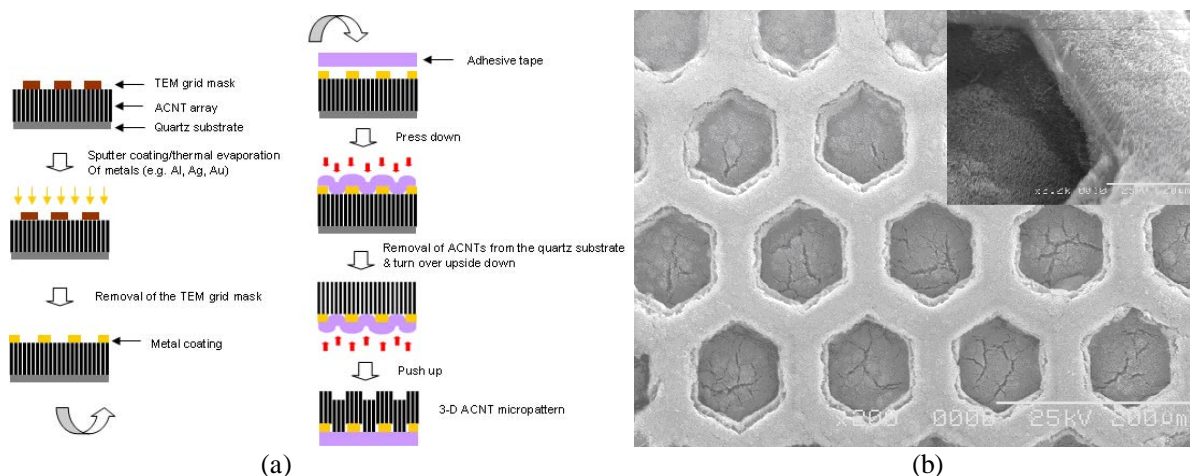
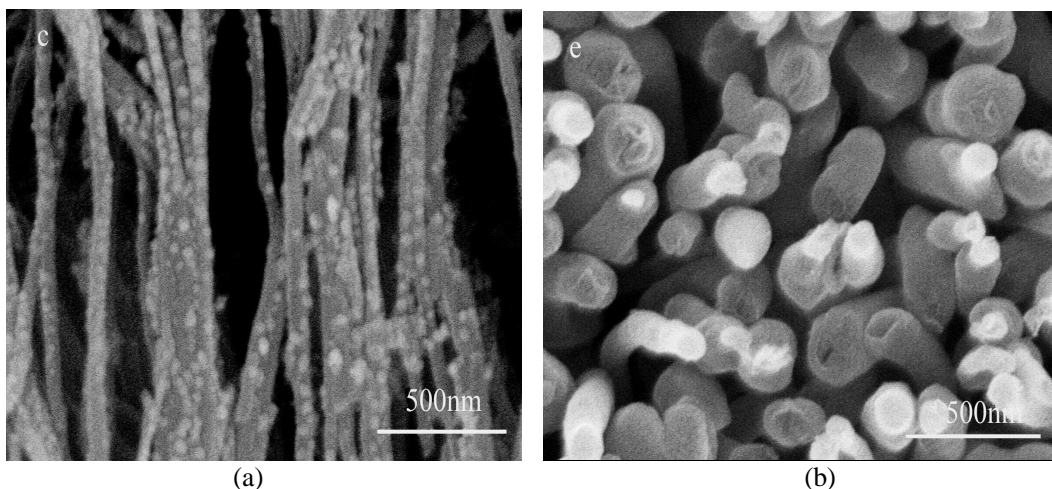


**Figure 5.** (a) Procedures for the fabrication of 3-D VA-MWNT micropatterns. (b) SEM micrographs of a 3-D VA-MWNT micropattern (Inset shows an enlarged view).

In addition, we have used the 3-D micropatterned aligned carbon nanotubes as electron emitters. We found a stepwise electron emission behavior for the 3-D micropatterned aligned carbon nanotubes and their 2-D counterparts prepared by plasma patterning. The observed stepwise electron emission was demonstrated to be rather versatile for multicomponent emitters, providing an effective means for developing multifunctional electron emitters with tailor-made field emission behaviors. With the recent rapid development in nanoscience and nanotechnology, these 3-D micropatterned and plasma-patterned aligned carbon nanotube electron emitters could be very useful in many multidimensional and multifunctional systems.

### 2.3. Controlled Preparation of Multi-dimensional Aligned Carbon Nanotubes Functionalized with Titanium Dioxide (*Adv. Mater.* **2007**, 19, 1239)

In this project, we have also developed a facile electrophoresis method for the effective preparation of aligned carbon nanotubes decorated with titanium dioxide ( $\text{TiO}_2$ ) nanoparticles/a coaxial coating layer (Figure 6a&b) and well-defined  $\text{TiO}_2$  nanomembranes. The  $\text{TiO}_2$ -based nanostructures thus produced were demonstrated to show fast photocurrent responses (Figure 6b). The unique photo-induced electron transfer properties make these  $\text{TiO}_2$ -functionalized aligned carbon nanotubes very attractive for many potential applications, particularly in dye-sensitized solar cells.



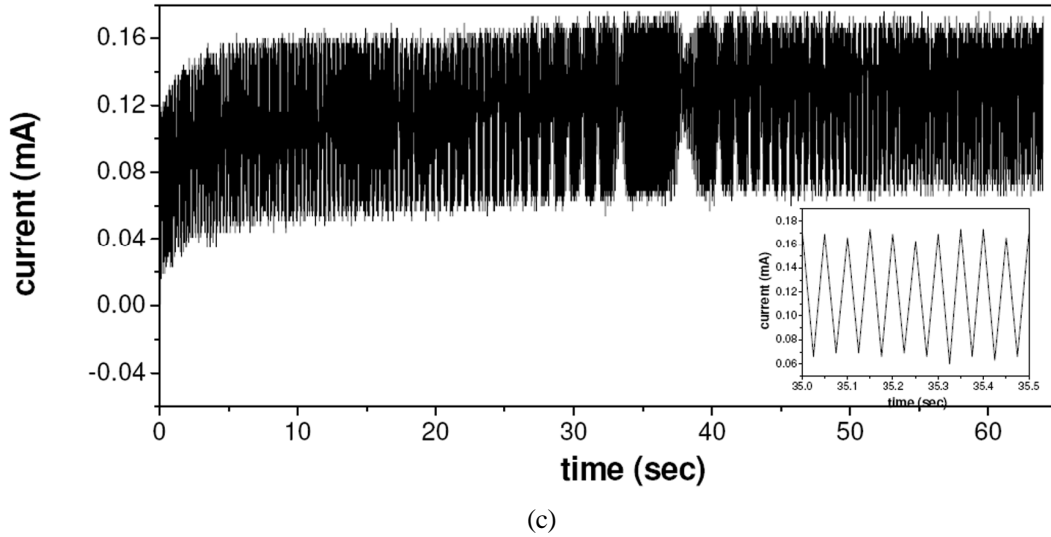


**Figure 6.** SEM images of (a) the VA-MWNTs after the electrophoresis deposition of  $\text{TiO}_2$  coating at 1 V for 15 min. (b) A top-view of the  $\text{TiO}_2/\text{VA-MWNT}$  coaxial nanowires after the electrophoresis deposition of  $\text{TiO}_2$  coating at 1 V for 30 min and heat treatment at  $600^\circ\text{C}$  in air for 30 min. (c) A typical photocurrent response for a  $\text{TiO}_2\text{-VACNT}$  coaxial nanowire film under UV exposure ( $\lambda = 254 \text{ nm}$ , 4 W) at room temperature. Inset shows an enlarged view for a small portion of the photocurrent response curve. The sample size is approximately  $1 \text{ cm}^2$ .

#### 2.4 Selective Growth of Semiconducting Aligned Single-walled Carbon Nanotubes (*Nano Lett.* **2008**, 8, 2682)

One of the critical aspects for developing the polymer-aligned carbon nanotube dispersed heterojunctions is to assemble polymers into aligned carbon nanotube arrays in a controllable manner. In such a multicomponent system, the overall functionality depends strongly on the semiconducting/metallic nature of the aligned carbon nanotubes as well as the precise location and structural characteristics of the infiltrated polymers. In this context, we have prepared *semiconducting* aligned single-walled carbon nanotubes through a selective nanotube growth. Subsequent infiltration of various polymers into the aligned carbon nanotube arrays opened up avenues for multifunctional applications, including polymer-aligned carbon nanotube photovoltaic cells.

*a) Selective Growth of Semiconducting Aligned Single-walled Carbon Nanotubes:* The major hurdle for the use of SWNTs in many electronic devices is the presence of both metallic and semiconducting carbon nanotubes in the *as-synthesized* nanotube samples. In order to avoid possible short circuit problem caused by metallic nanotubes and to improve the polymer-nanotube bulk heterojunction, it is critical to obtain pure semiconducting SWNTs for the construction of semiconductor devices from carbon nanotubes. Based on our previously-reported plasma-enhanced chemical vapor deposition (PECVD) combined with fast heating, we have demonstrated the selective growth of vertically-aligned *semiconducting* SWNTs by using fast heating and PECVD with only flow of  $\text{C}_2\text{H}_2$  at very low pressure of 30 mTorr. While the resultant nanotubes can be directly used for device applications, their semiconducting nature was clearly revealed by Raman spectroscopy. Figure 7 shows overall spectra of the *as-synthesized* VA-SWNTs and HiPco SWNTs by using 514nm laser (2.41eV), which has been demonstrated to give the best qualitative picture of metallic and semi-conducting nanotubes. For HiPco SWNTs, we can recognize the typical features of semi-conducting nanotubes over  $ca. 150\text{-}210 \text{ cm}^{-1}$  and metallic nanotubes over  $ca. 210\text{-}280 \text{ cm}^{-1}$  in the RMB region. We can also find the strong and broad Breit-Wigner-Fano (BWF) line shape for the  $\text{G}^-$  band associated with metallic nanotubes in Figure 7b. Unlike the HiPco SWNTs, however, the *as-synthesized* VA-SWNTs

show Raman characteristics dominated by semiconducting nanotubes in both RMB and G band regions. The resultant *semiconducting* SWNTs have been used directly for fabricating FET devices without any purification/separation to show comparable device performance to that of the SWNT thin film FETs after electrical breakdown of metallic nanotubes.

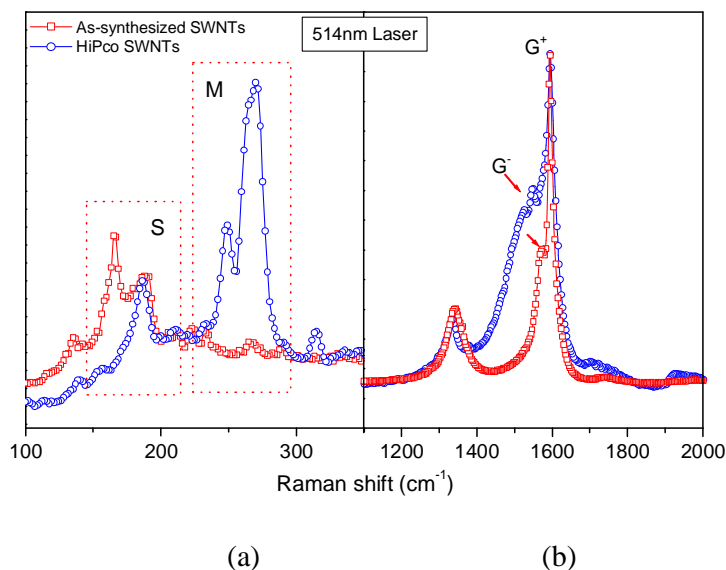


**Figure 7.** Typical Raman spectra of as-synthesized and HiPco SWNTs using laser wavelengths of 514 nm (Peaks within the squares marked with S and M correspond to the semiconducting and metallic SWNTs, respectively).

## 2.5 Smart Polymer and VA-CNTs Composites (*Chem. Commun.* **2008**, 1663; Cover page publication)

In order to construct the polymer-aligned carbon nanotube photovoltaic cells proposed in this project, a controlled infiltration of various polymers into the vertically-aligned carbon nanotube arrays is indispensable. In our further investigation on the aligned carbon nanotube and polymer nanocomposites for multifunctional materials and device applications, we have developed an effective and versatile method for tube-length-specific functionalization of carbon nanotubes through a controllable embedment of vertically-aligned carbon nanotubes into polymer matrices. In this context, we have demonstrated that the infiltration of temperature-responsive polymers (*e.g.*, PNIPAAm) into vertically-aligned carbon nanotube forests created synergetic effects, which provided the basis for the development of smart nanocomposite films with temperature-induced self-cleaning and/or controlled release capabilities. In this particular case, the infiltrated PNIPAAm chains underwent a temperature-induced rod-coil conformational transition at the lowest critical solution temperature (LCST  $\approx 32$  °C). The temperature-induced PNIPAAm chains collapse into or expand out from the nanotube gaps within the VA-MWNT forest, imparting the self-cleaning and controlled release properties to the PNIPAAm/VA-MWNT nanocomposite films (Figure 8). With so many stimuli (*e.g.* temperature, solvent, pH, photo, ionic, electrical)-responsive polymers already developed, and more to be synthesized, we can use the above concept to controlled/tuning the tube-tube distance within polymer-aligned carbon nanotube photovoltaic cells.

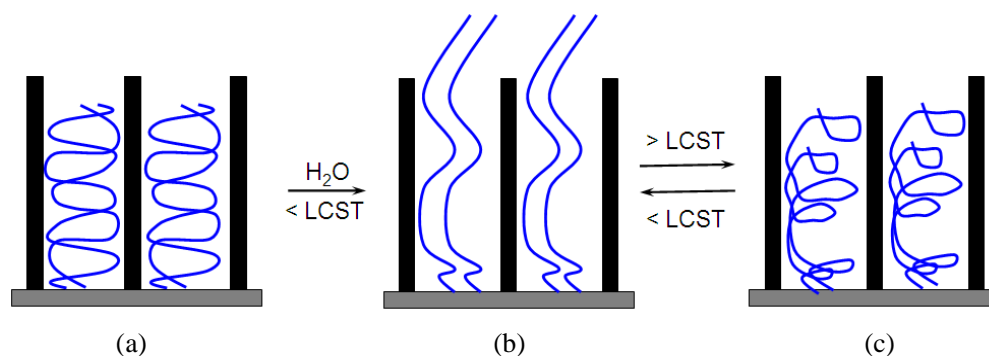


**Figure 8.** A schematic representation of the PNIPAAm/VA-MWNT film: (a & b) in the dry and wet state, respectively, at room temperature (20 °C), and (c) in a wet state at a temperature above LCST (~ 32 °C). For clarity, the infiltrated polymer mesh is represented by a few long polymer chains.

## B. SUMMARY OF ACCOMPLISHMENTS ON DEVICES

### 3 PHOTOVOLTAIC CELLS

Apart from the syntheses of photovoltaic-active macromolecules described above, some novel soluble liquid crystalline porphyrins that show discotic liquid crystalline (LC) phases homotropically-aligned into columns normal to the electrode were also supplied to us by Dr. Quan Li at Kent State University. We have also purchased liquid crystalline poly(2,5-bis(3-alkylthiophen-2-yl)thieno[3,2-b]thiophene) (PBTtT) from Merck. Photovoltaic cells based on these conjugated macromolecules and aligned carbon nanotubes were fabricated and characterized.

#### 3.1 Photovoltaic Cells from Dithienosilole-containing Polymers (Macromolecules 2009, 42, 114)

In order to investigate the potential use of polymers **12** and **13** (Scheme 1) in organic solar cells, bulk-heterojunction photovoltaic devices with the structure ITO/PEDOT-PSS(~35 nm)/polymer **12** or **13**:PCBM(1:1; 70–90 nm thick)/Al were fabricated. To determine the possible annealing effect on polymers **12** and **13** based devices, current-voltage measurements were taken while heating through periodic (10 °C) temperature increases *in-situ*. The comparison of PV performance before and after the thermal treatment was shown in Figure 9. The enhanced device performance is likely due to a possible thermal-induced reorganization of active components and subsequent improvements in charge mobility. The difference in the photovoltaic performance between polymer **12** and **13** may lie in the nature of the polymer backbone. The presence of internal electron donor-acceptor charge-transfer interaction and strong interchain interaction in polymer **13** resulted in extended absorption in the solar spectrum, and thus a better solar cell performance.

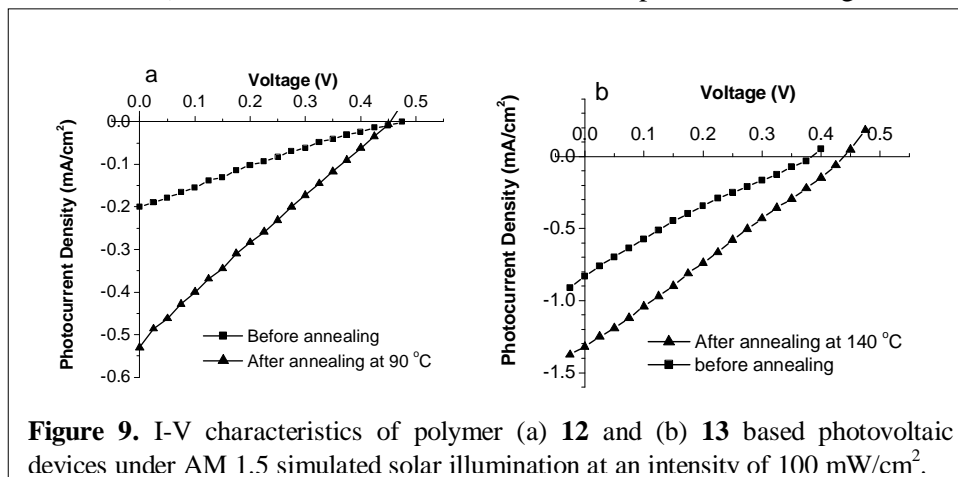


**Figure 9.** I-V characteristics of polymer (a) **12** and (b) **13** based photovoltaic devices under AM 1.5 simulated solar illumination at an intensity of 100 mW/cm<sup>2</sup>.

### 3.2 Photovoltaic Cells Based on D- $\pi$ -A Conjugated Copolymers (*J. Phys. Chem. B* **2008**, *112*, 2801)

Polymer photovoltaic cells with the structure of ITO/PEDOT:PSS (30 nm)/copolymer (Figure 2)-PCBM blend (70 nm)/Ca (8 nm)/Al(140 nm) have also been fabricated and characterized. The band gaps calculated from the UV-vis spectra, cyclic voltammetry scanning, and DFT modeling all indicated a narrowing band gap with the HOMO energy level increased with increasing the donor content in the polymer structure while the LUMO energy level remained relatively unchanged. It was thus found that the open-circuit voltage ( $V_{oc}$ ) increased (up to 0.93 V) with the decrease in the content of thiophene unit. Although the observed power conversion efficiency (PCE) for these unoptimized photovoltaic cells is still relatively low (up to 0.9%), the corresponding low fill factor (FF, 0.29) indicates considerable room for further improvement in the device performance. These results provided a novel concept for developing high  $V_{oc}$  photovoltaic cells based on donor- $\pi$ -acceptor conjugated copolymers by adjusting the donor/acceptor ratio.

### 3.3 Liquid Crystalline Polymers for Efficient Bilayer-Bulk-Heterojunction Solar Cells (*J. Phys. Chem. C* **2009**, *113*, 7892).

Comparing with low-molecular-weight porphyrins, the liquid crystalline poly(2,5-bis(3-alkylthiophen-2-yl)thieno[3,2-b]thiophene) (PBTTT) exhibits an interesting solubility in 1,2-dichlorobenzene or chlorobenzene (CB) - highly soluble in warm CB but insoluble at room temperature. This unique temperature-dependent solubility of PBTTT enabled us to spin-coat a CB solution of PBTTT at a high temperature (70 °C) and another overlaid polymer (*e.g.* poly[2-methoxy-5-(3,7-dimethyloctyloxy)]-1,4-phenylenevinylene), MDMO-PPV from the same solvent at room temperature without dissolving the preformed underlying PBTTT layer. This finding enabled us to construct the first bilayer-bulk-heterojunction devices based on a PBTTT:PCBM (1:2)/MDMO-PPV:[70]PCBM (1:4) active layer. The bilayer device exhibited an extended optical absorption over the solar spectrum and concentration gradient that enhanced charge carrier transport. Post-annealing the bilayer-bulk-heterojunction devices yielded a  $V_{oc}$  of 0.59 V,  $J_{sc}$ 's of 10.1-10.7 mA/cm<sup>2</sup>, FF of 0.50, and PCEs of 3.0-3.2 %, showing an increased  $J_{sc}$  and PCE by a factor of two with respect to their single layer counterparts (Figure 10). This study suggests that the bilayered device structure has distinct advantages for the development of highly efficient polymer solar cells.

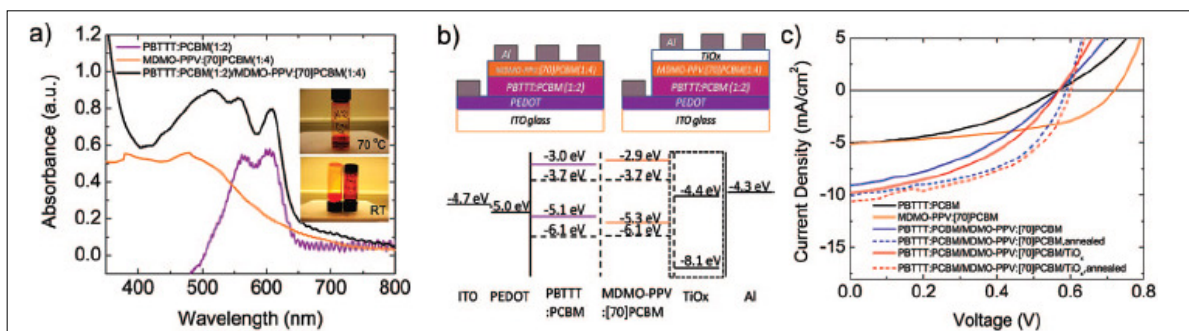


**Figure 10.** a) Optical absorption spectra for the blend films of PBTTT:PCBM (1:2 wt%), MDMO-PPV:[70]PCBM (1:4 wt%), and the bilayer blend film of PBTTT:PCBM (1:2 wt%)/MDMO-PPV:[70]PCBM (1:4 wt%). The insets show the digital photographs of PBTTT in CB at 70 °C (*up*) and PBTTT and MDMO-PPV in CB at room temperature (*bottom*). b) Schematic device configurations (*up*) of the bilayer-bulk-heterojunction solar cell with and without TiO<sub>x</sub>, and the associated energy level diagram (*bottom*). c) *J*-*V* characteristics of the single- and bi-layer bulk-heterojunction solar cells based on the PBTTT:PCBM (1:2 wt%) and MDMO-PPV:[70]PCBM (1:4 wt%) with and without TiO<sub>x</sub> before and after post-annealing.

### 3.4 Photovoltaic Cells Based on Liquid Crystalline Porphyrins (Appl. Phys. Lett. **2007**, 91, 253505)

As schematically shown in Figure 11, both bilayer- and bulk-heterojunction solar cells based on liquid crystalline porphyrins (donors) were fabricated by solution processing. In both cases, indium tin-oxide (ITO) glass coated with 30-nm-thick PEDOT:PSS was used as anode, and 15-nm-thick Ca capped with 150-nm-thick Al subsequently deposited under vacuum was employed as cathode. For photoactive layers in bilayer solar cells, a thin layer of porphyrin (80-nm thick) was spin-coated from its chlorobenzene solution onto the PEDOT/ITO anode, followed by thermally depositing C<sub>60</sub> (30-nm thick) onto the porphyrin layer under vacuum. In the bulk-heterojunction device, a blend thin film of the porphyrin and PCBM (1:1 w/w and ~230-250-nm thick spin-coated from a chlorobenzene solution) was used as the active layer.

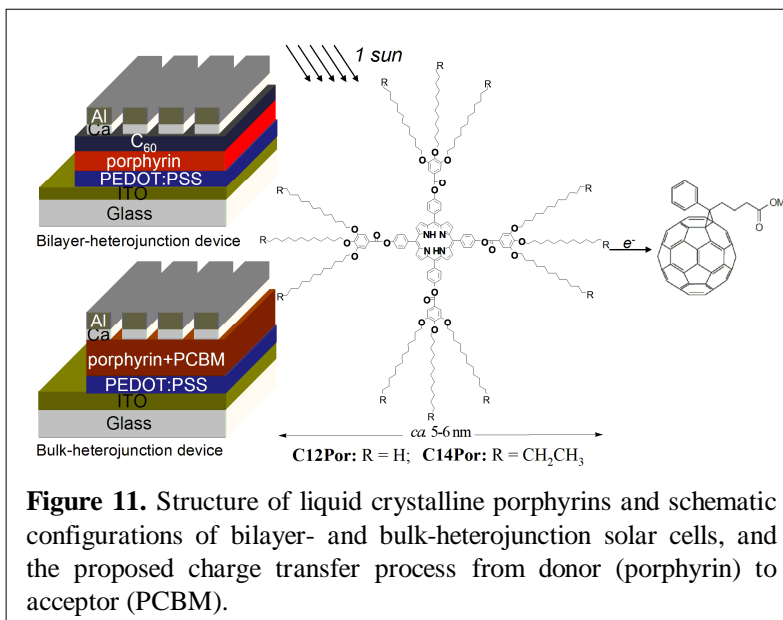


**Figure 11.** Structure of liquid crystalline porphyrins and schematic configurations of bilayer- and bulk-heterojunction solar cells, and the proposed charge transfer process from donor (porphyrin) to acceptor (PCBM).

Figure 12A(a&b) show typical current density vs. voltage ( $J$ - $V$ ) characteristics for bilayer solar cells based on C12Por and C14Por, respectively, before and after a post-annealing under the illumination of AM 1.5G, 100 mW/cm<sup>2</sup>. The *as-prepared* C12Por-based solar cell exhibited an open circuit voltage ( $V_{oc}$ ) of 0.495 V, a short circuit current density ( $J_{sc}$ ) of 0.400 mA/cm<sup>2</sup>, and power conversion efficiency ( $PCE$ ) of 0.070%. With an increased C-C linkage chain length, the  $V_{oc}$  of the *as-prepared* C14Por-based device decreased from 0.495 to 0.450 V with respect to the C12Por-based device, whereas the corresponding  $J_{sc}$  increased from 0.400 to 0.470 (mA/cm<sup>2</sup>). The observed decrease in  $V_{oc}$  with a concomitant increase in  $J_{sc}$  with increasing the C-C linkage chain length can be attributed to the reduced recombination losses of the “excitons/carriers” through enhanced charge localization in the C14Por device. Figure 12A shows that the post-annealing induced a more than 100% increase in both  $J_{sc}$  and  $PCE$ , presumably due to the thermally-induced alignment of porphyrin layer. The homeotropic alignment of the porphyrins could not only provide the most efficient pathway for hole conduction along the columnar axis crossing the device thickness, but also offer the largest area to the incident light for optimized light harvesting.

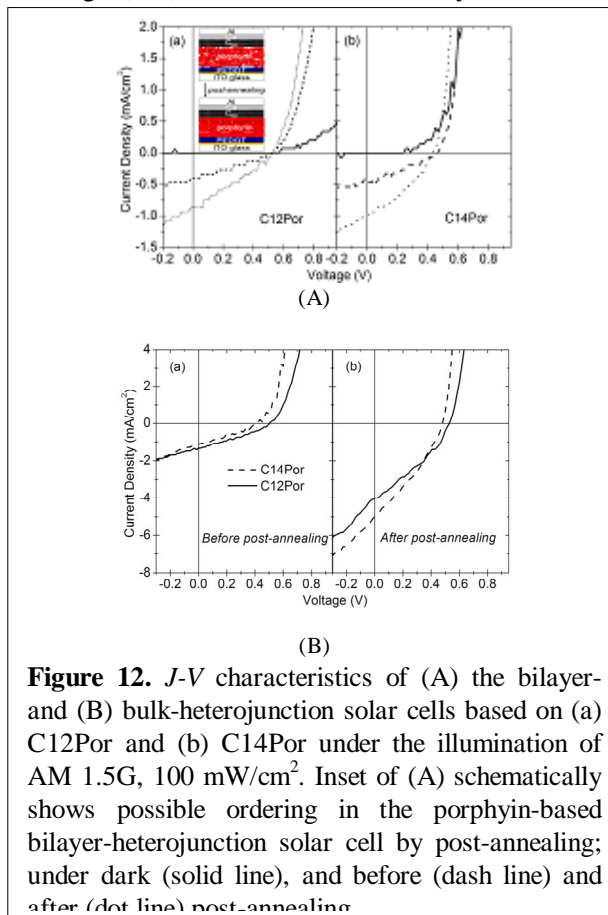
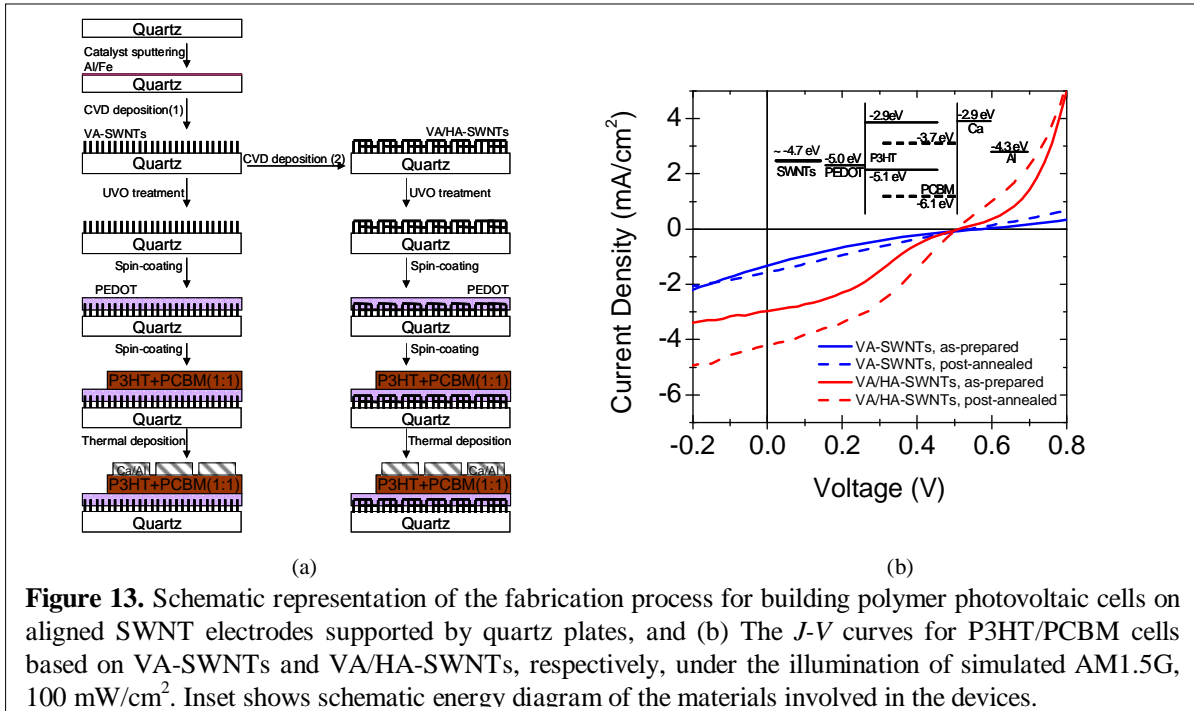


**Figure 12.**  $J$ - $V$  characteristics of (A) the bilayer- and (B) bulk-heterojunction solar cells based on (a) C12Por and (b) C14Por under the illumination of AM 1.5G, 100 mW/cm<sup>2</sup>. Inset of (A) schematically shows possible ordering in the porphyrin-based bilayer-heterojunction solar cell by post-annealing; under dark (solid line), and before (dash line) and after (dot line) post-annealing

As shown in Figure 12B(a&b),  $J_{sc}$ s and  $PCE$ s of the bulk-heterojunction solar cells were also improved significantly with about 200–300% and 300–400% increase, respectively, by the post-annealing treatment due, once again, to the thermally-induced alignment of the porphyrins – though a full homeotropic alignment may be difficult in the blend system with PCBM interdispersed between the porphyrin liquid crystal columns. After the post-annealing, the C12Por-based solar cell achieved a  $J_{sc}$  of 3.990 mA/cm<sup>2</sup> and a  $PCE$  of 0.712%, while the C14Por-based solar cell exhibited a  $J_{sc}$  of 5.02 mA/cm<sup>2</sup> and a  $PCE$  of 0.775%. This study provides an evidence for enhancing the photovoltaic performance by homeotropically aligning photo-active liquid crystalline porphyrins into columns normal to the electrode.

### 3.5 Photovoltaic Cells Based on Vertically-aligned Carbon Nanotubes

The very promising results from the homeotropically-aligned liquid crystalline porphyrins described above prompted us to build organic bulk heterojunction solar cells by infiltrating photovoltaic active polymers into the vertically-aligned carbon nanotube arrays. Despite the great difficulty in eliminating the short circuit problem, photovoltaic effects were achieved in the P3HT/PEDOT-based solar cells using *short* VA-SWNTs (~1  $\mu$ m long) grown on a quartz plate as anode. In order to enhance the sheet conductivity, we have also grown horizontally-aligned metallic nanotubes between the nanotube gaps in the VA-SWNT “forest” (designed as: VA-/HA-SWNTs). We have prepared photovoltaic cells by spin-coating a buffer layer (~ 100 nm) of PEDOT and a photoactive layer (~ 180 nm) of P3HT:PCBM (1:1, wt/wt) blend onto VA-SWNTs or VA/HA-SWNTs electrode on a quartz plate, followed by thermal depositing Ca (15 nm)/Al (150 nm) cathode under vacuum (Figure 13a). Figure 13b shows the current density-voltage curves for the P3HT/PCBM cells based on VA-SWNTs and VA/HA-SWNTs, respectively. From the energy diagram shown in the inset of Figure 13b, it is clear that both the VA-SWNTs and VA/HA-SWNTs (~ -4.7 eV) act as a hole-collection electrode in each of the devices. The photovoltaic cell based on the VA/HA-SWNT electrode exhibits much improved performance with respect to its counterpart on the VA-SWNT electrode. The same  $V_{oc}$  (0.51 V) was obtained for both devices, suggesting that the  $V_{oc}$  is related to the work function of the PEDOT layer rather than that of the SWNTs. The decreased  $J_{sc}$ ,  $FF$  and  $PCE$  for the device on VA-SWNTs are attributable to their higher sheet resistance than that of VA/HA-SWNTs. Although the photovoltaic performance for these unoptimized photovoltaic cells using aligned



SWNTs on quartz plates as anode are still not sufficiently high, this study demonstrated the novel concept for building polymer solar cells onto the aligned nanotube arrays on *non-conducting* (non-ITO) substrates. With so many multifunctional aligned CNTs of controlled structure and surface characteristics already developed in our group, and more to be synthesized, there should be considerable room for improving the performance of the aligned CNT solar cells.

### C. OTHER ENERGY-RELATED DEVICES

#### 4.1 DNA-enhanced Multilayer White Polymer Light-emitting Diodes (LEDs) (*Appl. Phys. Lett.* **2008**, 92, 251108)

White polymer LEDs are promising for energy-efficient flat lighting applications. Using a thin film of deoxyribonucleic acid-cetyltrimethylammonium (DNA-CTMA) complex as a hole-transporting/electron-blocking layer, we have developed a sequential solution-processing approach for constructing multilayer (up to five layers) white polymer light-emitting diodes, incorporating the poly(9,9-dioctylfluorene-2,7-diyl)/poly[2-methoxy-5(2'-ethyl-hexyloxy)-1,4-phenylene vinylene] emissive layer. These devices were demonstrated to show a low turn-on voltage ( $\sim 5$  V), high efficiency (10.0 cd/A), and high brightness (10500 cd/m<sup>2</sup>) with an improved white-color stability (Figure 14).

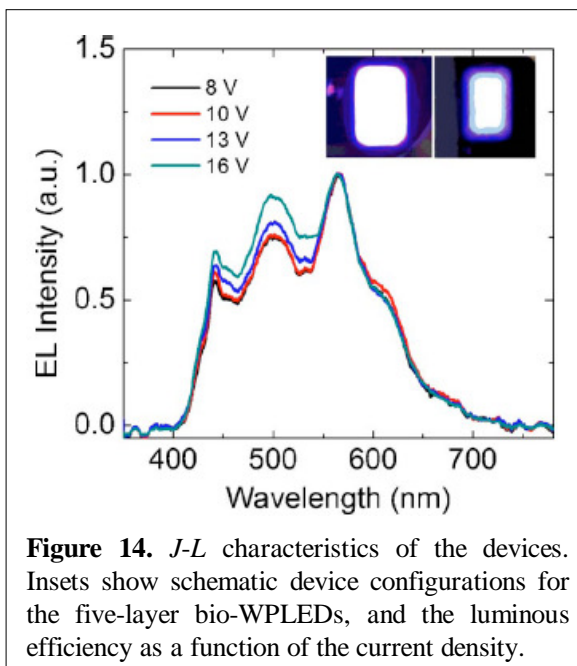


**Figure 14.** *J-L* characteristics of the devices. Insets show schematic device configurations for the five-layer bio-WPLEDs, and the luminous efficiency as a function of the current density.

#### 4.2 Quantum Dot Light-emitting Diodes (QD-LEDs) (*ACS Nano* **2009**, 3, 737)

Owing to their narrow bright emission band, broad size-tunable emission wavelength, superior photostability, and excellent flexible-substrate compatibility, light-emitting diodes based on quantum dots (QD-LEDs) are currently under intensive research and development for multiple consumer applications including flat-panel displays and flat lighting. However, their commercialization is still

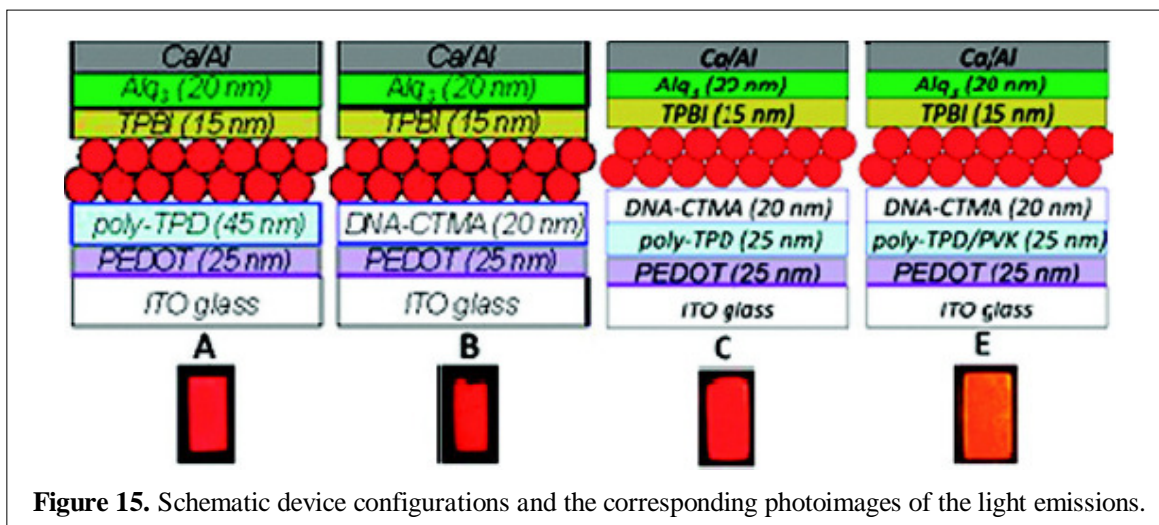


**Figure 15.** Schematic device configurations and the corresponding photoimages of the light emissions.

precluded by the slow development to date of efficient QD-LEDs as even the highest reported efficiency of 2.0% cannot favorably compete with their organic counterparts. We reported QD-LEDs with a record high efficiency (~4%), high brightness (~6580 cd/m<sup>2</sup>), low turn-on voltage (~2.6 V), and significantly improved color purity by simply using deoxyribonucleic acid (DNA) complexed with cetyltrimethylammonium (CTMA) (DNA2CTMA) as a combined hole transporting and electron-blocking layer (HTL/EBL). This, together with controlled thermal decomposition of ligand molecules from the QD shell, represents a novel combined, but simple and very effective, approach toward the development of highly efficient QD-LEDs with a high color purity ([http://academic.udayton.edu/LimingDai/nano.2009.63%20\(Highlight%20QD-LED\)9.pdf](http://academic.udayton.edu/LimingDai/nano.2009.63%20(Highlight%20QD-LED)9.pdf)).

#### 4.3 N-doped Carbon Nanotube Arrays as An Efficient Cathode for Fuel Cells (*Science* **2009**, 323, 760)

The oxygen reduction reaction (ORR) at the cathode of fuel cells plays a key role in controlling the performance of a fuel cell, and efficient ORR electrocatalysts are essential for practical applications of the fuel cells. The ORR can proceed either through a four-electron process to combine oxygen with electrons and protons directly, when coupled with oxidation on the anode, to produce water as the end product, or a less efficient two-step two-electron pathway involving the formation of hydrogen peroxide ions as an intermediate. Platinum has long been regarded as the most efficient ORR catalyst, but their large-scale commercial application has been largely precluded by its high cost. Besides, the Pt-based electrode also suffers from its susceptibility to time-dependent drift and CO deactivation. We found that vertically-aligned nitrogen-containing carbon nanotubes (VA-NCNTs) produced by pyrolysis of iron(II) phthalocyanine (FePc, a metal heterocycle molecules containing nitrogen), in either the presence or absence of additional NH<sub>3</sub> vapor, could be used as effective ORR electrocatalysts even after a complete removal of the residual Fe catalyst by electrochemical purification. These metal-free VA-NCNTs were shown to catalyze a four-electron ORR process with a much higher electrocatalytic activity, lower overpotential (*i.e.*, the difference between thermodynamic and formal potentials), smaller crossover

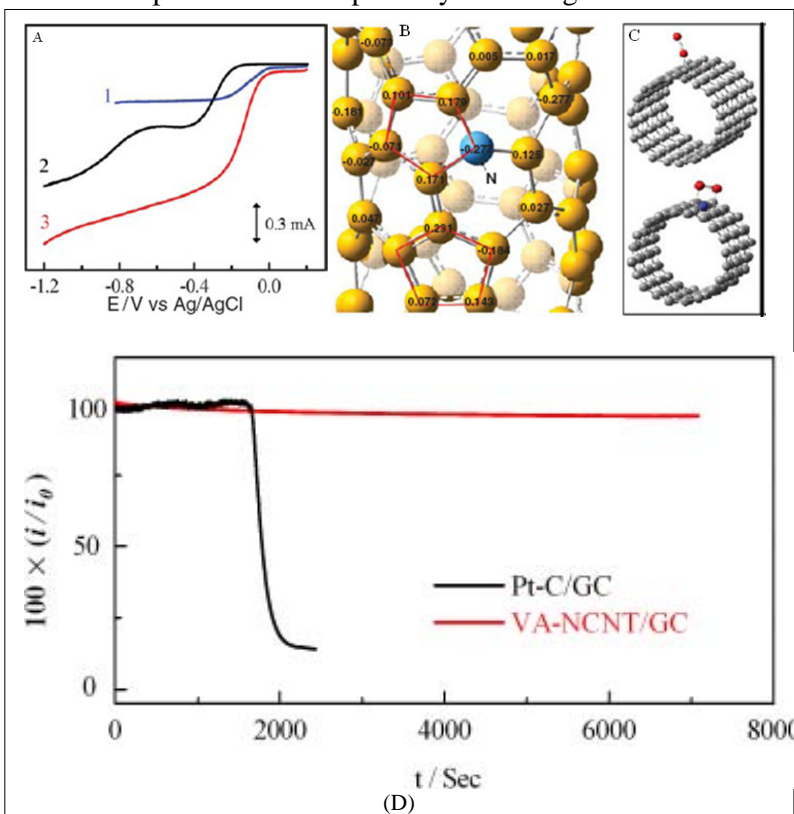


**Figure 16.** (A) Rotating ring electrode voltammograms for oxygen reduction in air-saturated 0.1 M KOH at the Pt (curve 1), vertically-aligned nitroge-free carbon nanotube (VA-CCNT, curve 2), and VA-NCNT (curve 3) electrodes. (B) The calculated charge density distribution for the NCNTs. (C) Schematic representations of possible adsorption modes of an oxygen molecule at the CCNTs (top) and the NCNTs (bottom). (D) The CO-poison effect on the *i-t* Chronoamperometric response for the Pt-C/GC and VA-NCNT/GC electrodes upon the addition of ~9% CO (v/v) into the electrochemical cell from the 55 mL/min CO and 550 mL/min O<sub>2</sub> mixture gas

effect, and better long-term operation stability even than that of commercially available or similar platinum-based electrodes (C2-20, 20% platinum on Vulcan XC-72R; E-TEK) in alkaline electrolytes (Figure 16). Our quantum mechanics calculations show that each nitrogen atom attracts electrons from neighbouring carbon atoms, which are then topped up by more electrons flowing from the anode. When an oxygen molecule hits the cathode, therefore, there is a ready supply of electrons to facilitate the oxygen reduction reaction.

### 3.4 Gecko-foot-mimetic Aligned Carbon Nanotube Dry Adhesives for Energy Management (Science 2008, 322, 238)

The unusual ability of gecko lizards to climb on any vertical surface and hang from a ceiling with one toe has inspired scientific research for centuries. Recent studies revealed that the driving force for holding gecko lizards on a surface arises from the strong van der Waals (vdW) forces ( $\sim 10 \text{ N}\cdot\text{cm}^{-2}$ ) induced by countless aligned microscopic elastic hairs called setae ( $3\text{-}130 \mu\text{m}$  in length) and spatulae ( $0.2\text{-}0.5 \mu\text{m}$  in diameter) on a gecko's foot. This finding has prompted many researchers to fabricate microarrays of polymer pillars to mimic gecko feet. Due to the inability to synthetically mimic the fine structure of geckos' setae and spatulae, however, these polymeric dry adhesives (with a maximum achievable adhesive force of  $\sim 3 \text{ N}\cdot\text{cm}^{-2}$ ) are not comparable to the gecko feet. Subsequent work on macroscopic arrays of vertically-aligned carbon nanotubes set new records for the carbon nanotube dry adhesives. The small nanotube diameter, together with a  $\pi$ -conjugated carbon

surface, allowed vertically-aligned carbon nanotube arrays to have an imitate contact with the substrate and a strong vdW force for each of the contacts, leading to an enhanced adhesion force for the vertically-aligned carbon nanotube dry adhesives. By using rationally-designed hierarchical structure of the vertically-aligned carbon nanotubes (VA-MWNTs) with a coiled/entangled nanotube top strands, we have developed gecko-foot-mimetic dry adhesives with a record high shear adhesion force (along the surface it is stuck to) of  $\sim 100 \text{ N}\cdot\text{cm}^{-2}$  - 10 times more stickier than natural gecko feet. Unlike other gecko-inspired glues using a carpet of straight nanotubes/nanowires without the curly

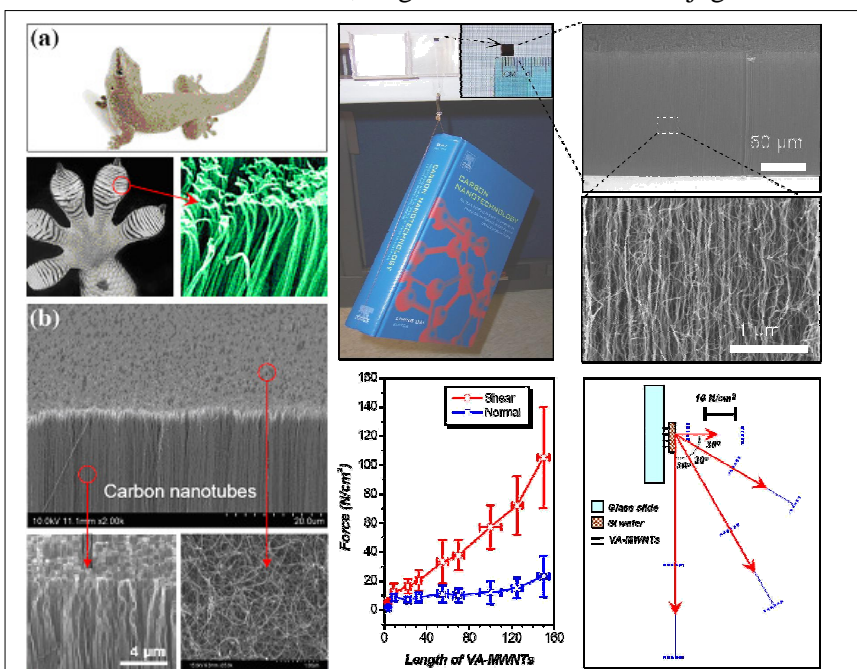


**Figure 2.** (Left panel) Typical images for the gecko-foot elastic hairs and vertically-aligned carbon nanotubes. (Right panel) A small piece of the as-grown VA-MWNT film ( $4 \times 4 \text{ mm}^2$ ) was finger pressed from the Si side onto a vertically positioned glass slide. A book of 1480 g was clung onto a thin wire that was pre-glued on the back side of the Si substrate. An overall adhesion force of  $90.7 \text{ N/cm}^2$  was calculated. The shear adhesion force is typically several times stronger than the corresponding normal adhesion force at a constant nanotube length over about 10 mm. To elucidate the angular-dependence of the adhesion forces, we measured the pull-off force in various pull-away directions. The decrease in the pull-off force with increasing pull-away angle indicates that the shear adhesion force is much stronger than the normal adhesion force.

entangled top, this new nanotube mimic gecko foot when it is pulled in a direction parallel to its surface, the tangled portion of the nanotubes becomes aligned in contact with the surface to dramatically increase the contact area between the nanotubes and the surface, and hence maximizing the shear adhesion force. When lifted off the surface in a direction normal to the substrate surface, as one would peel a piece of Scotch tape vertically, the nanotubes lose contact point by point, minimizing the normal adhesion force. This anisotropic force distribution ensures strong binding along the shear direction and easy lifting in the normal direction, allowing alternatively binding-on and lifting-off over various substrates for simulating the walking of a living gecko.

This discovery could lead to various applications, ranging from low-tech fridge magnets to holding together electronics or even the airplane parts. For instance, rather than soldering components into electronic devices, the parts could be easily held together by using the new adhesive. Computers and laptops could be made to disperse heat from their circuits without the need for additional heat sinkers. As a dry adhesive, the carbon nanotube material would also have many uses in space where there is a vacuum and traditional kind of adhesives dry out. They can also be used to create wall/rock climbing robots, super-grip tires, and rapid repairs for various systems. In one of our relevant studies (*Adv. Mater.* **2007**, *19*, 3844), we used tailor-made vertically-aligned single-walled carbon nanotube arrays (VA-SWNTs) to mimic gecko feet. The single-walled carbon nanotube dry adhesive is nearly three times more sticker than natural gecko feet with additional thermal and electrical management capabilities. For instance, the vertically-aligned SWNT dry adhesives showed fairly reversible semiconducting behaviors under load and an excellent thermal resistance due to the unique thermal and electric properties intrinsically associated with SWNTs. These unusual multifunctionalities should make the VA-SWNT dry adhesives very attractive for diverse applications, including their use as electrically and thermally conductive adhesives for electrical/thermal (energy) management. These research activities, along with those mentioned in other sections in this report, should provide a large body of information that allows Air Force to enhance the efficiency of photovoltaic cells and to design novel energy-related systems to accomplish missions that are impossible with current devices and methods.

## II. JOURNAL PAPERS PUBLISHED FROM THIS PROJECT WITH ACKNOWLEDGEMENTS TO THE AFOSR GRANT AND PATENT APPLICATIONS

### JOURNAL PUBLICATIONS

1. Patil, A.; Ohashi, T.; Buldum, A.; Dai, L.  
“Controlled preparation and electron emission properties of 3-Dimensional micropatterned aligned carbon nanotubes”  
*Appl. Phys. Lett.* **2006**, *89*, 103103.
2. Sun, Q.; Dai, L.; Zhou, X.; Li, L.; Li, Q.  
“Bilayer- and bulk-heterojunction solar cells using liquid crystalline porphyrins as donors by solution processing”  
*Appl. Phys. Lett.* **2007**, *91*, 253505.
3. Yang, Y.; Qu, L.; Dai, L.; Kang, T.S.; Durstock, M.  
“Electrophoresis coating of titanium oxide onto aligned carbon nanotubes for controlled syntheses of photoelectronic nanomaterials”  
*Adv. Mater.* **2007**, *19*, 1239.
4. Qu, L.; Dai, L.  
“Direct growth of multicomponent micropatterns of vertically-aligned single-walled carbon nanotubes interposed with their multi-walled counterparts on Al-activated iron substrates”  
*J. Mater. Chem.* **2007**, *17*, 3401 (Cover page publication).

5. Yang, J.; Qu, L.; Zhao, Y.; Zhang, Q.; Dai, L.; Baur, J.W.; Maruyama, B.; Vaia, R.A.; Shin, E.; Murray, P.T.; Luo, H.; Guo, Z.-X.  
“Multicomponent and multidimensional carbon nanotube micropatterns by dry contact transfer”  
*J. Nanosci. Nanotechnol.* **2007**, 7, 1573.
6. Chang, D.W.; Dai, L.  
“Luminescent amphiphilic dendrimers with oligo(*p*-phenylene vinylene) core branches and oligo(ethylene oxide) terminal chains: syntheses and stimuli-responsive properties”  
*J. Mater. Chem.* **2007**, 17, 364.
7. Dai, L.  
“Electrochemical Sensors Based On Architectural Diversity of the  $\pi$ -Conjugated Structure: Recent Advancements from Conducting Polymers to Carbon Nanotubes”  
*Aust. J. Chem. – Internal. J. Chem. Sci.* **2007**, 60, 472.
8. Liu, J.; Dai, L.; Baur, J.W.  
“Multi-Wall Carbon Nanotubes for Flow-Induced Voltage Generation”  
*J. Appl. Phys.* **2007**, 101, 064312.
9. Liao, L.; Dai, L.; Smith, A.; Durstock, M.; Lu, J.; Ding, J.; Tao, Y.  
“Photovoltaic-active dithienosilole-containing polymers”  
*Macromolecules* **2007**, 40, 9406.
10. Qu, L.; Chen, W.; Dai, L.; Roy, A.; Benson-Tolle, T.  
“Polymer and aligned carbon nanotube nanocomposites and nanodevice”  
*SAMPE J.* **2007**, 43(6), 38.
11. Chang, D.W.; Dai, L.  
“Photo-induced formation and self-assembling of gold nanoparticles in aqueous solution of amphiphilic dendrimers with oligo(*p*-phenylene vinylene) core branches and oligo(ethylene oxide) terminal chains”  
*Nanotechnology* **2007**, 18, 365605.
12. Chen, W.; Qu, L.; Chang, D.; Dai, L.; Ganguli, S.; Roy, A.  
“Vertically-aligned carbon nanotubes infiltrated with temperature-responsive polymers: smart nanocomposite films for self-cleaning and controlled release”  
*Chem. Commun.* **2008**, 163 (Cover page publication).
13. Qu, L.; Dai, L.; Stone, M.; Xia, Z.; Wang, Z.L.  
“Carbon nanotube arrays with strong shear binding-on and easy normal lifting-off”  
*Science* **2008**, 322, 238.
14. Yang, R.; Qin, Y.; Dai, L.; Wang, Z.L.  
“Flexible charge-pump for power generation using laterally packaged piezoelectric-wires”  
*Nature Nanotechnology* **2009**, 4, 34.
15. Bergeson, J.D.; Etzkorn, S.J.; Murphey, M.B.; Qu, L.; Yang, J.B.; Dai, L.; Epstein, A.J.  
“Iron nanoparticle driven spin-valve behavior in aligned carbon nanotube arrays”  
*Appl. Phys. Lett.* **2008**, 93, 172505.
16. Li, L.; Kang, S.-W.; Harden, J.; Sun, Q.; Zhou, X.; Dai, L.; Jakli, A.; Kumar, S.; Li, Q.  
“Nature inspired light-harvesting liquid crystalline porphyrins for organic photovoltaics”  
*Liquid Crystals* **2008**, 35, 233.
17. Peng, Q.; Qu, L.; Dai, L.; Park, K.; Vaia, R.  
“Asymmetrically charged carbon nanotubes by controlled functionalization”  
*ACS Nano* **2008**, 2, 1833.
18. Qu, L.; Du, F.; Dai, L.  
“Preferential syntheses of semiconducting vertically-aligned single-walled carbon nanotubes for direct use in FETs”  
*Nano Lett.* **2008**, 8, 2682.
19. Chakrabarti, S.; Gong, K.; Dai, L.

- “Structural evaluation along the nanotube length for super-long vertically-aligned double-walled carbon nanotube arrays”  
*J. Phys. Chem. C* **2008**, *112*, 8136.
20. Sun, Q.; Chang, D.W.; Dai, L.; Grote, J.; Naik, R.  
 “Multilayer white polymer light-emitting diodes with deoxyribonucleic acid-cetyltrimethylammonium complex as hole-transporting/electron-blocking layers”  
*Appl. Phys. Lett.* **2008**, *92*, 251108.
  21. Peng, Q.; Park, K.; Lin, T.; Durstock, M.; Dai, L.  
 “Donor- -acceptor conjugated copolymers for photovoltaic applications: Tuning the open-circuit voltage by adjusting the donor/acceptor ratio”  
*J. Phys. Chem. B* **2008**, *112*, 2801.
  22. Qu, L.; Peng, Q.; Dai, L.; Spinks, G.; Wallace, G.; Baughman, R.H.  
 “Carbon nanotube electroactive polymer materials: opportunities and challenges”  
*Mater. Res. Soc. Bull.* **2008**, *33*, 215.
  23. Chen, W.; Qu, L.; Chang, D.; Dai, L.; Ganguli, S.; Roy, A.  
 “Vertically-aligned carbon nanotubes infiltrated with temperature-responsive polymers: Smart nanocomposite films for self-cleaning and controlled release”  
*Chem. Commun.* **2008**, 163 (Cover page publication).
  24. Gong, K.; Du, F.; Xia, Z.; Dustock, M.; Dai, L.  
 “Nitrogen-doped carbon nanotube arrays with high electrocatalytic activities for oxygen reduction”  
*Science* **2009**, *323*, 760.
  25. Lu, W.; Qu, L.; Henry, K.; Dai, L.  
 “High performance electrochemical capacitors from aligned carbon nanotube electrodes and ionic liquid electrolytes”  
*J. Power Source* **2009**, *189*, 1270.
  26. Sun, Q.; Subramanyam, G.; Dai, L.; Check, M.; Campbell, A.; Naik, R.; Grote, J.; Wang, Y.  
 “Highly efficient quantum-dot light-emitting diodes with DNA-CTMA as the hole-transporting/electron-blocking layer”  
*ACS Nano* **2009**, *3*, 737.
  27. Sun, Q.; Park, K.S.; Dai, L.  
 “Liquid crystalline polymers for highly-efficient bilayer bulk-heterojunction solar cells”  
*J. Phys. Chem. C* **2009**, *113*, 7892.

#### JOINT PATENT APPLICATION WITH AFRL

- Qu, L.; Stone, M.; Dai, L.  
 “Functionalized aligned carbon nanotubes for dry adhesive applications”  
*Provisional Patent Application.*

### III. PERSONNEL SUPPORT

#### PROJECT PARTICIPANTS

##### *Senior Personnel*

Liming Dai (PI, UD)

##### *Post-doctors*

QingJiang Sun (Full time, UD)

Qiang Peng (Part time, UD)

Liangti Qu (Part time, UD)

#### *Graduate Student*

Kuyson Park (Part-time, UD)

#### *AFRL Collaborators*

Michael Durstock (WPAFB)

James Grote (WPAFB)

Morley Stone (WPAFB)

Throughout the project, close collaboration was maintained with Dr. Michael Durstock at AFRL/MLBP in Dayton. Dr. Dai had worked together with Dr. James Grote on the light-emitting diodes and with Dr. Morley Stone on the CNT dry adhesives. Dr. Dai and his team will continue to work closely together with Dr. Durstock's team to build a strong and long-term collaboration on energy initiatives to meet the Air Force needs.

## **IV. SIGNIFICANCE TO AIR FORCE AND CIVILIAN TECHNOLOGY CHALLENGES**

Recent developments in military applications have placed renewed demands for new and improved high performance flexible power systems with significant improvements in weight to volume ratios and extraordinarily energy generation and storage capacities. This project brought together expertise and resources available at UD and AFRL. The outcome of the project directly supported the mission of AFOSR and AFRL and has contributed significantly towards strengthening the national capability for research and development of next generation flexible power systems, including organic solar cells, by: 1) providing Air Force with a scientific rationale that led to innovations in the design of lightweight, flexible solar cells for Air Force applications, 2) providing a body of information that allowed Air Force to design flexible power systems to accomplish missions that are impossible with current devices and methods, 3) training graduate and post-doctoral students who assumed major responsibilities in critical defense- and civilian-related power system R&D, 4) bringing together multidisciplinary expertise and resources in the area of materials synthesis, characterization, device construction, and system integration from both UD and AFRL, and 5) enhancing academic collaboration with Air Force laboratories and other DoD national laboratories. The interests of this project to Air Force has been clearly evidenced by a substantial amount of the proposed work that has been carried out in the Wright-Patterson Air Force Research Laboratory in close collaboration with several AFRL researchers.

The outcomes of this project should also provide an opportunity for the domestic energy industry to create new jobs and strengthens the U.S. economy. This will further enhance our position to capture the economic and military benefits emerging from developments in this field. Our work has received numerous commentaries appeared in scientific, business, and popular press (please see: "Events & News" at <http://academic.udayton.edu/LimingDai/>), including *Science daily*, *Nature Nanotechnology*, *Nature Chemistry*, *Chemical Engineering News*, *New Scientist*, *MIT Technology Review*, *Green Car Congress*, *Market Chronicle*, and *Energy Industry Today*, *Washington Business Journal*, *U.S. Politics Today*, *Fox News*, *ABC* and *Reuters*. Our reported and patented technologies are envisioned to be transformative and having a large impact on the energy field, and their repercussions are continuing.

## **V. INTERACTIONS/TRANSITIONS**

The PI and team members have presented the results from this project at many national and international conferences, including:

## **2009**

Invited talk at The 238<sup>th</sup> American Chemical Society Meeting, Washington DC, August, 2009.

Invited talk at the AFRL Nanotechnology Materials and Devices Workshop, Cincinnati, June, 2009.

Talk at the Joint Navy Air Force Organic/Hybrid Solar Cell Research Program Review, National Harbor, MD, May, 2008.

Invitation talk at The 6th Annual USAF-Taiwan Nanoscience Workshop, San Francisco, April, 2009

Invited talk at The Guadalupe Workshop (Organized by AFRL, NASA Johnson Space Center and the Smalley Institute of Rice University), Texas, April, 2009.

Invited talk at The 237<sup>th</sup> American Chemical Society Meeting, Salt Lake City, March, 2009.

Invited talk at the Ohio Innovation Summit, Dayton, April, 2009.

## **2008**

Invited talk at the 2008 International Symposium on Materials for Enabling Nanodevices (ISMEN2008), National Cheng Kung University, Tainan, Taiwan, September, 2008.

Invited talk at the 2008 SPIE Optics and Photonics: Nanoscience and Engineering, San Diego, August, 2008.

Invited talk at The 2nd International Conference on Advanced Nano Materials (ANM 2008), Aveiro, Portugal, June, 2008.

Talk at 2008 Polymer Chemistry and Polymer Composite Contractor's Meeting, AFOSR, Maryland, May, 2008.

## **2007**

Invited talk at the 2007 AIChE Annual Meeting, Salt Lake City, November, 2007.

Invited talk at the (International) Society for Advancement of Material and Process Engineering (SAMPE) Annual Conference, Cincinnati, October, 2007.

Invited talk at the 172<sup>nd</sup> Rubber Division Meeting, Cleveland, October, 2007.

Invited talk at The Technology Cooperation Program (TTCP, involving the defense departments of the US, UK, Canada, Australia, New Zealand), The US Naval Academy, Annapolis Maryland, September, 2007.

Plenary talk at the SPIE *Optics and Photonics*, San Diego, August, 2007.

Invited talk at the American Chemical Society Meeting, Boston, August, 2007.

Invited talk at the 4<sup>th</sup> International Conference on Materials for Advanced Technology, Singapore, July, 2007.

Invited talk at the ANTEC 2007, Cincinnati, May, 2007.

Invited talk at the Central Regional Meeting of the American Chemical Society, Cincinnati, May, 2007.

Invited talk at the AFRL Biotronic Workshop, Hawaii, May, 2007.